Supplementary Material

Calculation of the Shape

Finding the solution that best fits gravity and radio occultation measurements

Assumption of barotropic system: atmosphere perfectly stratified with no horizontal variations.

Zonal winds rotate on cylinders penetrating deeper into the planet than the region probed by radio occultations; interpretations of Jupiter's odd zonal harmonics suggest that the observed winds may penetrate around 3000 km inside the planet[1][2].

Hence, the obtained dynamical height represents the height of barotropic surfaces.

On the other side, radio occultations measure the shape of isopycnic surfaces.

In the case of a barotropic atmosphere the two shapes coincide[3].

[1] *Guillot, Tristan et al. (2018). "A suppression of differential rotation in Jupiter's deep interior". In: Nature 555.7695, pp. 227–230.*

[2] *Kaspi, Y ea et al. (2018). "Jupiter's atmospheric jet streams extend thousands of kilometres deep". In: Nature 555.7695, pp. 223–226.*

[3] *Lindal, G. F., Sweetnam, D. N., & Eshleman, V. R. (1985). The atmosphere of Saturn-an analysis of the Voyager radio occultation measurements. Astronomical Journal (ISSN 0004-6256), vol. 90, June 1985, p. 1136-1146. NASA-supported research., 90, 1136-1146.*

Data

- **Gravity coefficients**: Updated coefficients from Juno's nominal mission midpoint[1];
- **ZWPs**: Profiles from Voyager 2 (1979) and Hubble/WFC3 (2009–2019)[2][3];
- **Radio occultations**: Data from Juno's extended mission.

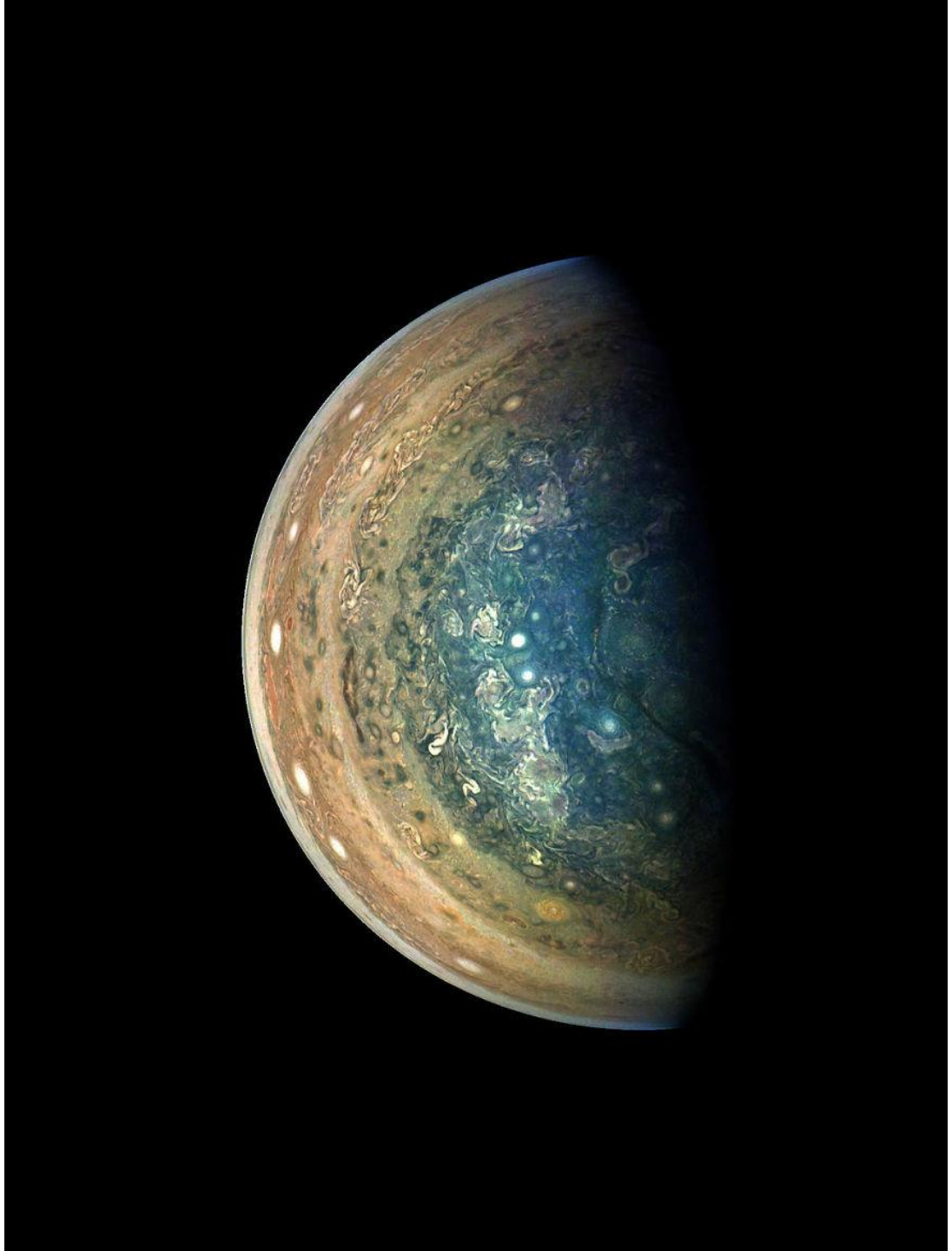

[1] Durante, D et al. (2020). "Jupiter's gravity field halfway through the Juno mission". In: Geophysical Research Letters 47.4, e2019GL086572.
[2] Limaye, Sanjay S (1986). "Jupiter: New estimates of the mean zonal flow at the cloud level". In: Icarus 65.2-3, pp. 335–352.
[3] Tollefson, Joshua et al. (2017). "Changes in Jupiter's Zonal Wind Profile preceding and during the Juno mission". In: Icarus 296, pp. 163–178.
[4] Wong, Michael H et al. (2020). "High-resolution UV/optical/IR imaging of Jupiter in 2016–2019". In: The Astrophysical Journal Supplement Series 247.2, p. 58.

Gravity Coefficients

Zonal harmonics	Values
$J_2 \times 10^{-6}$	14,696.5735 ± 0.0017
$J_3 \times 10^{-6}$	-0.0450 ± 0.0033
$J_4 \times 10^{-6}$	-586.6085 ± 0.0024
$J_5 \times 10^{-6}$	-0.0723 ± 0.0042
$J_6 \times 10^{-6}$	34.2007 ± 0.0067
$J_7 \times 10^{-6}$	0.120 ± 0.012
$J_8 \times 10^{-6}$	-2.422 ± 0.021
$J_9 \times 10^{-6}$	-0.113 ± 0.036
$J_{10} \times 10^{-6}$	0.181 ± 0.065
$J_{11} \times 10^{-6}$	0.016 ± 0.111
$J_{12} \times 10^{-6}$	0.062 ± 0.190

Durante, D., Parisi, M., Serra, D., Zannoni, M., Notaro, V., Racioppa, P., ... & Bolton, S. J. (2020). Jupiter's gravity field halfway through the Juno mission. Geophysical Research Letters, 47(4), e2019GL086572.

Zonal Winds

Voyager 2 (1979)
HST 2009
HST 2012
HST 2015 (OPAL)
HST 2016 (OPAL)
HST 2016 (PJ03)
HST 2017 (11 January)
HST 2017 (02 February)
HST 2018
HST 2019
Our synthetic wind

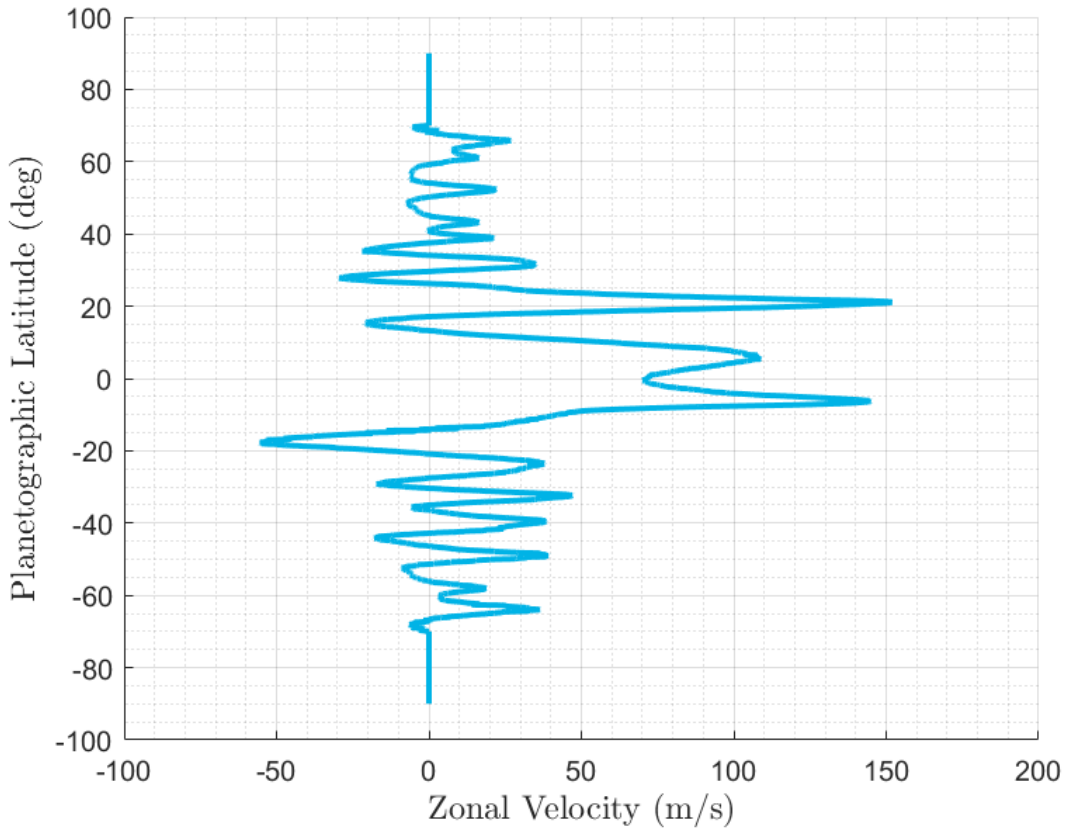

Radio Occultations

Experiment	Estimated uncertainty (km)	Experiment	Estimated uncertainty (km)
PJ54I	2.7	PJ54E	1
PJ60I	-	PJ60E	1
PJ61I	1	PJ61E	-
PJ62I	1	PJ62E	1
PJ63I	0.5	PJ63E	1
PJ64I	0.32	PJ64E	0.8
PJ65I	0.25	PJ65E	1
PJ66I	1	PJ66E	1
PJ67I	1	PJ67E	1

Work in progress
Not included

Method

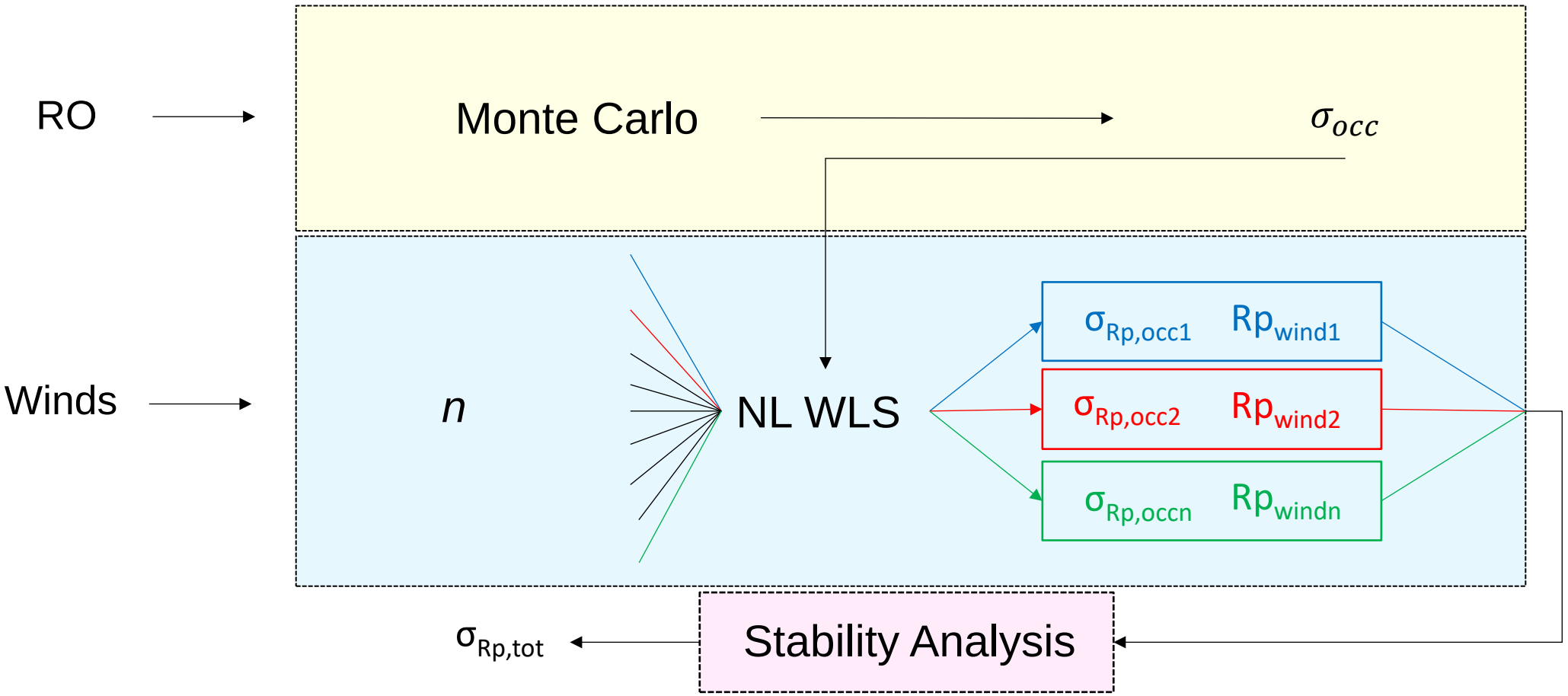
RO
Monte Carlo
σ_{occ}
Winds
n
NL WLS
$\sigma_{Rp,occ1}$ Rp_{wind1}
$\sigma_{Rp,occ2}$ Rp_{wind2}
$\sigma_{Rp,occn}$ Rp_{windn}
$\sigma_{Rp,tot}$
Stability Analysis

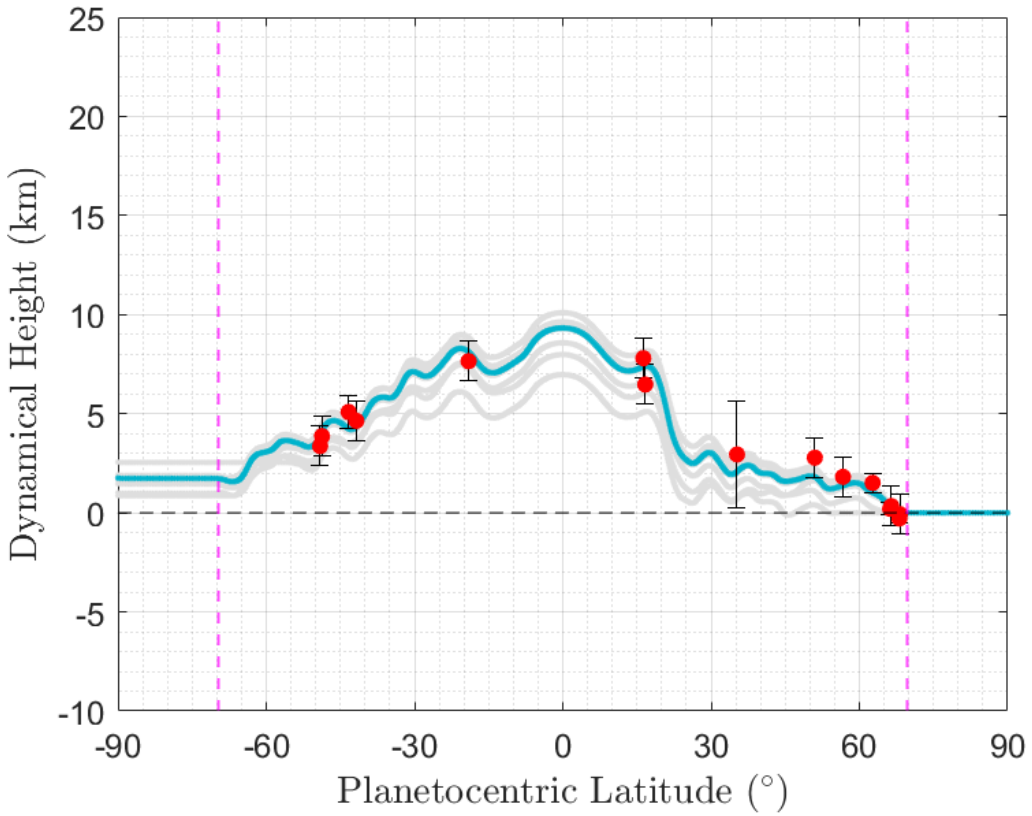
Dynamical Height (km)
25
20
15
10
5
0
-5
-10
-90
-60
-30
0
30
60
90
Planetocentric Latitude (°)

Uncertainties in the Shape

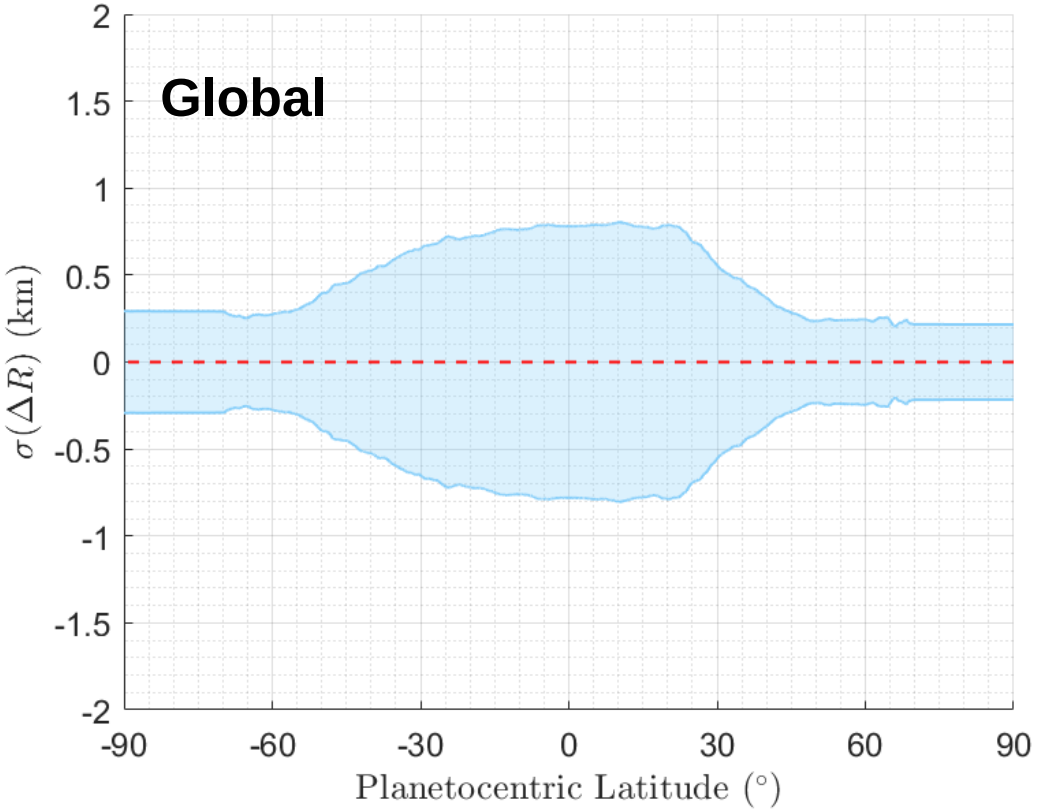

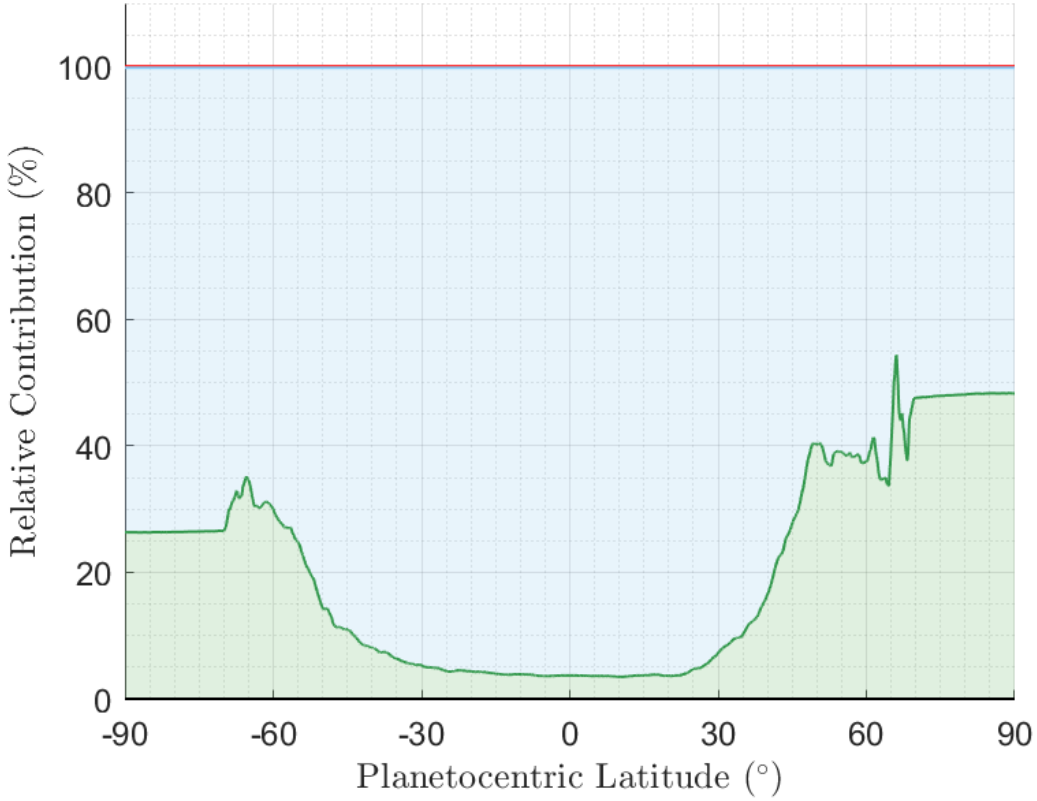

Radio Occultations

The spacecraft transmits at a frequency f_s in its rest frame, and the signal at the antenna is received at a frequency f_a in the rest frame of the DSN station.

The two frequencies are related by

$$\frac{f_a}{f_s} = \left(\frac{1 - \frac{\hat{\boldsymbol{n}}_a \cdot \boldsymbol{v}_a}{c}}{1 - \frac{\hat{\boldsymbol{n}}_s \cdot \boldsymbol{v}_s}{c}}\right)\left(\frac{1 - \frac{2U(\boldsymbol{r}_s)}{c^2} - \frac{v_s^2}{c^2}}{1 - \frac{2U(\boldsymbol{r}_a)}{c^2} - \frac{v_a^2}{c^2}}\right)^{\frac{1}{2}}$$

Relativistic Doppler | Gravitational effects

Schinder, P. J., Flasar, F. M., Marouf, E. A., French, R. G., Anabtawi, A., Barbinis, E., & Kliore, A. J. (2015). A numerical technique for two-way radio occultations by oblate axisymmetric atmospheres with zonal winds. Radio Science, 50(7), 712–727. doi:10.1002/2015rs005690.

Radio Occultations

Eikonal Equation (differentially rotating atmosphere)

$$\frac{d\hat{n}}{ds} = \frac{1}{n}[\nabla n - \hat{\boldsymbol{n}}(\hat{\boldsymbol{n}} \cdot \nabla n)] - \frac{n^2 - 1}{c}\left[\frac{d\boldsymbol{V}}{ds} - (\hat{\boldsymbol{n}} \cdot \nabla)\boldsymbol{V} + \hat{\boldsymbol{n}} \times (\nabla \times \boldsymbol{V})\right]$$

Wind shear Rotation Vorticity

Doppler residual frequency

$$f_{res}(t) = f_a(t) - f_v(t)$$

with $f_v(t)$ frequency expected in the vacuum (extracted from eq. 1 once $f_s(t)$ is given).

Radio Occultations

Eikonal Equation (differentially rotating atmosphere)

$$\frac{d\hat{n}_x}{ds} = n^{-1}\left(\left(1 - 2n\hat{\mathbf{n}}\cdot\frac{\mathbf{V}}{c} - (\hat{n}_x)^2 + 2n\frac{V_x}{c}\hat{n}_x\right)\frac{\partial n}{\partial x} - \left(\hat{n}_x - 2n\frac{V_x}{c}\right)\hat{n}_y\frac{\partial n}{\partial y} - \left(\hat{n}_x - 2n\frac{V_x}{c}\right)\hat{n}_z\frac{\partial n}{\partial z}\right.$$
$$\left. - \frac{1}{c}(n^2-1)\hat{\mathbf{n}}\cdot\frac{\partial \mathbf{V}}{\partial x} + (n^2-1)(\hat{\mathbf{n}}\cdot\nabla)\frac{V_x}{c}\right),$$

$$\frac{d\hat{n}_y}{ds} = n^{-1}\left(\left(1 - 2n\hat{\mathbf{n}}\cdot\frac{\mathbf{V}}{c} - (\hat{n}_y)^2 + 2n\frac{V_y}{c}\hat{n}_y\right)\frac{\partial n}{\partial y} - \left(\hat{n}_y - 2n\frac{V_y}{c}\right)\hat{n}_x\frac{\partial n}{\partial x} - \left(\hat{n}_y - 2n\frac{V_y}{c}\right)\hat{n}_z\frac{\partial n}{\partial z}\right.$$
$$\left. - \frac{1}{c}(n^2-1)\hat{\mathbf{n}}\cdot\frac{\partial \mathbf{V}}{\partial y} + (n^2-1)(\hat{\mathbf{n}}\cdot\nabla)\frac{V_y}{c}\right),$$

$$\frac{d\hat{n}_z}{ds} = n^{-1}\left(\left(1 - 2n\hat{\mathbf{n}}\cdot\frac{\mathbf{V}}{c} - (\hat{n}_z)^2 + 2n\frac{V_z}{c}\hat{n}_z\right)\frac{\partial n}{\partial z} - \left(\hat{n}_z - 2n\frac{V_z}{c}\right)n_y\frac{\partial n}{\partial y} - \left(\hat{n}_z - 2n\frac{V_z}{c}\right)\hat{n}_x\frac{\partial n}{\partial x}\right.$$
$$\left. - \frac{1}{c}(n^2-1)\hat{\mathbf{n}}\cdot\frac{\partial \mathbf{V}}{\partial z} + (n^2-1)(\hat{\mathbf{n}}\cdot\nabla)\frac{V_z}{c}\right).$$

Schinder, P. J., Flasar, F. M., Marouf, E. A., French, R. G., Anabtawi, A., Barbinis, E., & Kliore, A. J. (2015). A numerical technique for two-way radio occultations by oblate axisymmetric atmospheres with zonal winds. Radio Science, 50(7), 712–727. doi:10.1002/2015rs005690.

Radio Occultations

How a radio occultation analysis works:

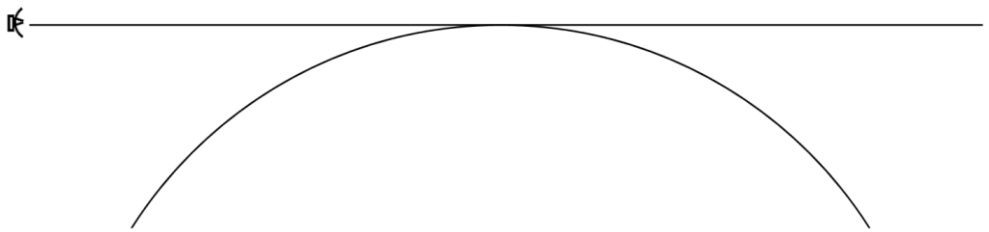

First ray → straight line connecting spacecraft to Earth. Ray periapsis sets the top of the atmosphere.

Schinder, P. J., Flasar, F. M., Marouf, E. A., French, R. G., Anabtawi, A., Barbinis, E., & Kliore, A. J. (2015). A numerical technique for two-way radio occultations by oblate axisymmetric atmospheres with zonal winds. Radio Science, 50(7), 712–727. doi:10.1002/2015rs005690.

Radio Occultations

How a radio occultation analysis works:

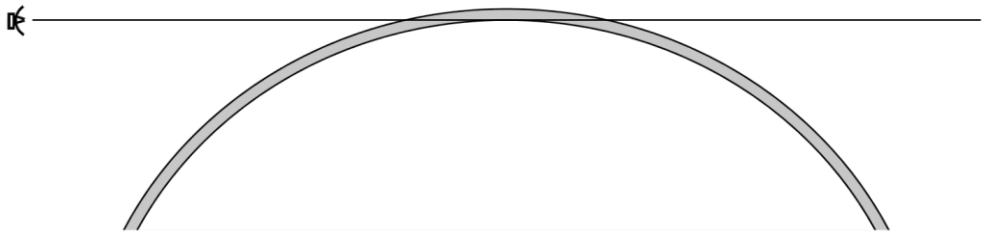

Assume the interior is filled with a substance of constant dN/dU, and find dN/dU and $\hat{\boldsymbol{n}}_{\boldsymbol{s}}$ so that:

$$\text{(i) } f(\hat{\boldsymbol{n}}_{\boldsymbol{s}}) - f_a(t) = 0$$

$$\text{(ii) } \hat{\boldsymbol{n}}_{\boldsymbol{e}}(\hat{\boldsymbol{n}}_{\boldsymbol{s}}, dN/dU) - \hat{\boldsymbol{n}}_{\boldsymbol{a}}(t) = 0$$

Schinder, P. J., Flasar, F. M., Marouf, E. A., French, R. G., Anabtawi, A., Barbinis, E., & Kliore, A. J. (2015). A numerical technique for two-way radio occultations by oblate axisymmetric atmospheres with zonal winds. Radio Science, 50(7), 712–727. doi:10.1002/2015rs005690.

Radio Occultations

How a radio occultation analysis works:

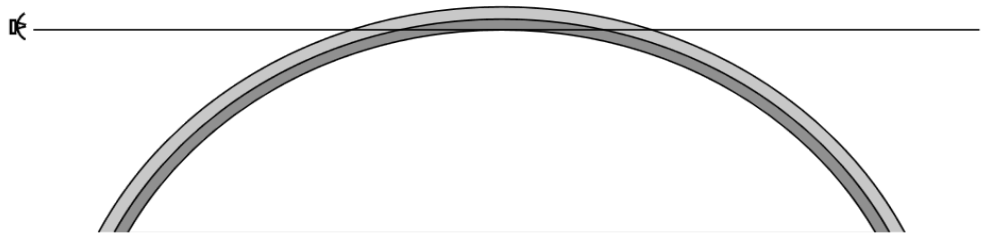

Once the solution is found to a specific accuracy, we mark the inner layer of a shell by the minimum value of the potential U along the ray. The interior of this shell is now assigned the value of dN/dU_i as a fixed value, with i index of the correspondent shell → integrate over U_i to obtain $N(U)$

Schinder, P. J., Flasar, F. M., Marouf, E. A., French, R. G., Anabtawi, A., Barbinis, E., & Kliore, A. J. (2015). A numerical technique for two-way radio occultations by oblate axisymmetric atmospheres with zonal winds. Radio Science, 50(7), 712–727. doi:10.1002/2015rs005690.

Radio Occultations

How a radio occultation analysis works:

Once the solution is found to a specific accuracy, we mark the inner layer of a shell by the minimum value of the potential U along the ray. The interior of this shell is now assigned the value of dN/dU_i as a fixed value, with i index of the correspondent shell → integrate over U_i to obtain $N(U)$

↓

$N(U)$ + atmospheric composition + refractivity per molecule of each component → $\rho(U)$

↓

$\rho(U)$ + hydrostatic equilibrium + equation of state → P-T vertical profile

Schinder, P. J., Flasar, F. M., Marouf, E. A., French, R. G., Anabtawi, A., Barbinis, E., & Kliore, A. J. (2015). A numerical technique for two-way radio occultations by oblate axisymmetric atmospheres with zonal winds. Radio Science, 50(7), 712–727. doi:10.1002/2015rs005690.

Radio Occultations

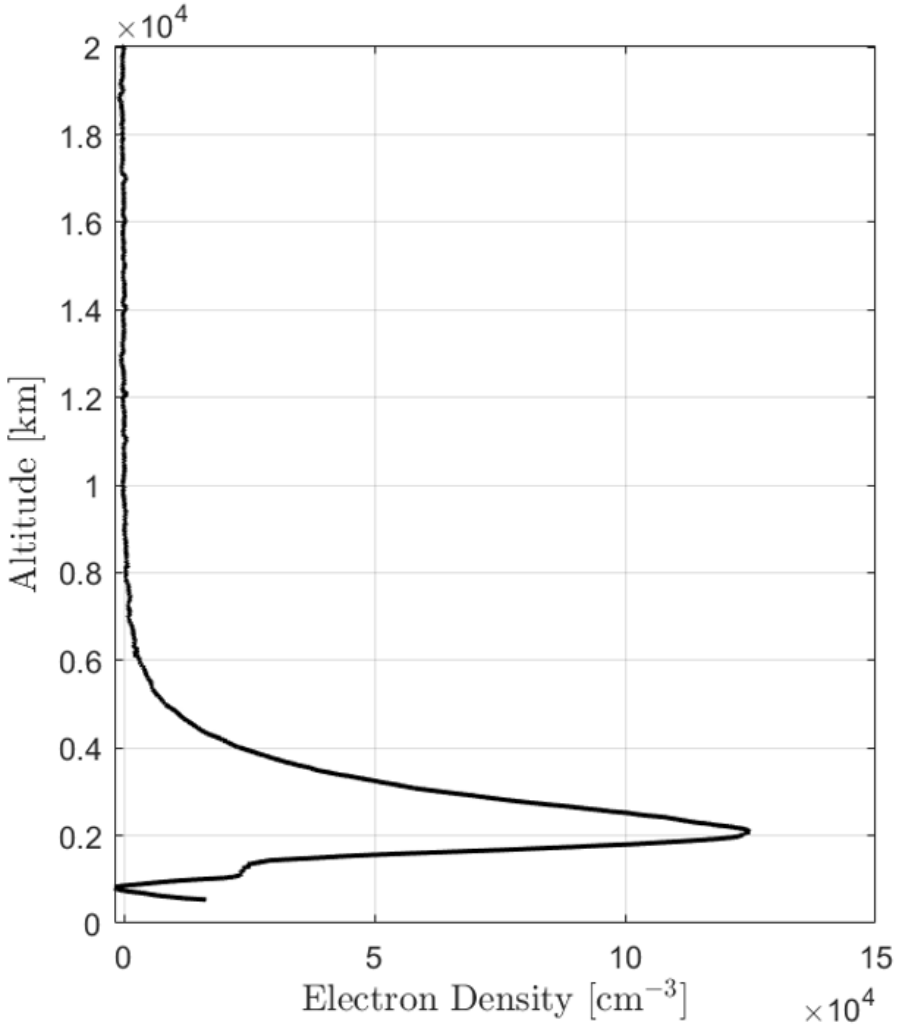

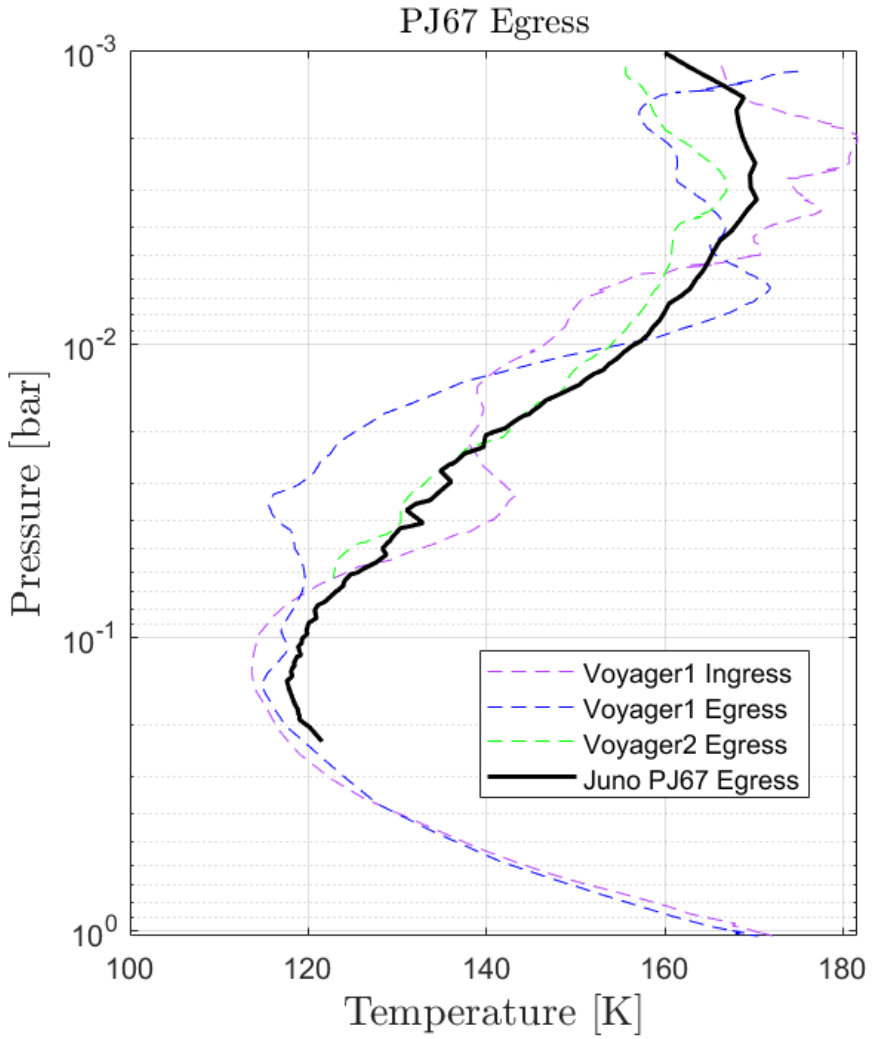

Juno-Jupiter Occultations

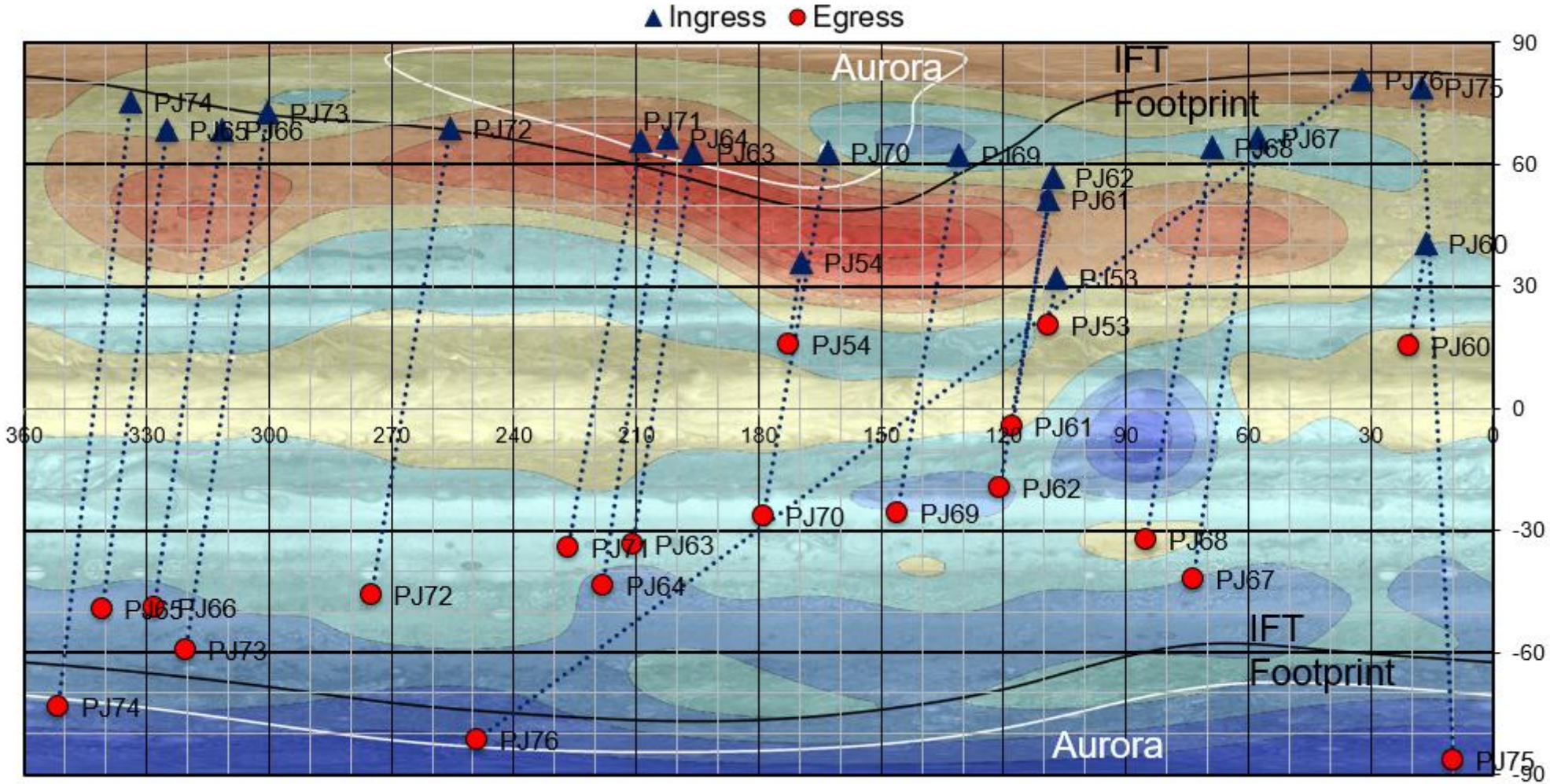

Diagram courtesy Marty Brennan, Juno Mission Planning